Automated measurement of carotid angle with use of CT images

Nusret Demir *[*1] ID, **Serkan Demir** [2] ID

[1] *Akdeniz University, Department of Space Science and Technologies, Antalya, Türkiye*
[2] *Medical Sciences University Sancaktepe Research and Application Hospital, Istanbul, Türkiye*

Keywords

Medical Image Processing
Photogrammetry
CT
Neurology
Stroke

Abstract

Carotid stenosis is an important etiological factor in the forming of ischemic stroke. The weight of stroke which is formed as a result of extracranial internal carotid artery stenosis or occlusion differs according to the location, size of interaction, collateral supply, and the mechanisms those cause interact. Therefore, it is important to measure the narrowness of the carotid with the calculation of the bifurcation angle. In this study, CT cross-sectional image sequences are used. The images are unsupervised classified, and the carotid veins are identified with the boundaries and centers of the clusters. Then, the angles are calculated with three center points of the veins from successive images. The center point of the calculation is from the vein which has the maximum area difference between one of the successive images. The results are evaluated using 5 samples with visual interpretation regarding the position and the correctness of the three successive images which have maximum area jump.

1. Introduction

There are two types of Carotis Communis vessels that carry blood to the brain: Carotis interna and Carotis externa. The narrowing of the carotid arteries is referred to as carotid artery disease, also known as carotid artery stenosis. In most cases, plaques made of fatty substances and cholesterol are to blame for the carotid's narrowness. The risk of stroke is greatly enhanced if the carotid arteries are occluded. An expanded version of Demir and Demir's study [1] is presented here.

The narrowing of the carotid Interna usually develops after separation from the carotid communities, and the main cause is turbulence flood in this section. Although the death rate has decreased in the recent decade, ischemic paralysis remains a major medical problem. Despite the use of thrombolysis and other treatment options in acute ischemia paralysis, prevention is the most successful approach. The data utilized to determine risk factors are based on epidemiological studies that were conducted at random [2].

As shown in Figure 1, the blood is supplied into the human brain via the right and left internal carotid artery which is split from the two-sided common carotis artery [3]. The focal neurological situations based on cerebrovascular diseases are called as stroke [4]. Carotis stenosis is an important etiological factor in the forming of ischemic stroke [5]. According to the studies which use Doppler USG, more than 50% of the automatically Carotis stenosis is seen in 4-5% of patients who are elder than 65 years old [6]. The risk of stroke is increased by the degree of stenosis [7].

The weight of a stroke which is formed as a result of extracranial internal carotid artery stenosis or occlusion differs according to the location, size of interaction, collateral supply, and the mechanisms that cause interaction. Stroke causes demoralization and morbidity for the patients [8-10]. Stroke is the third most seen cause of death, and it is the first human disorder [6]. Thus, for detection of narrowness at an early stage has become of high interest to many researchers.

The researches rely mainly on the determination of carotid bifurcation parameters, such as volume, position, etc.

Dix et al. [10] identify the ideal measurement methods and acquisition parameters for CT angiography of carotid bifurcation. They use various measurement

approaches to compare SSD images (Shaded surface display), MIP (Maximum Intensity Projection), magnified axial images, and axial images. They offer automation but end with the benefits of CT imaging.

A deformable tubular 3D Non-Uniform Rational B-Splines (NURBS) model is used by Suinesiaputra et al. [11] to design and validate a method for automatic segmentation of the carotid artery lumen from volumetric MR Angiographic (MRA) images. They perform automatic cross-sections from the artery for the carotid measurements using MR imaging with NURBS 3D model output.

Using stereoscopic PIV (Particle Image Velocimetry) measurements, Kefayati and Poepping [12] describe the disrupted flow in the stenosed carotid artery.

Fisher [13] investigates the effect of the geometry of carotid arteries into the flow characteristics. He shows that the apoptotic and biochemical changes of upstream carotid plaque are closely linked to the development of stroke symptoms. Similarly, Stroud et.al [14] perform a numerical analysis of flow through a severe stenosis carotid artery bifurcation to investigate the geometry of the vessels.

There is research that computes the blood flow in the vessels using numerical models.

Cebral et al. [15] created a technique for creating accurate patient-specific finite element models of carotid artery blood flow. With a tubular deformable model along each artery branch, they used MR data to build anatomical models. At two points below and above the bifurcation, they calculated the flow velocities. They made it possible to describe the created model's flow patterns.

Tan et. al. [16] develop turbulence models to predict blood flow patterns in the carotid artery and calculate the oscillating vessel Wall stresses. The model is MR image-based and simulated the wall shear stress.

In order to determine the mechanical properties resulting from the influence of the lipid core and calcification within a plaque, Wong et. al. [17] design a numerical simulation that reflects the distribution and structure of plaque via 3D blood-vessel modeling.

Gul and Bernhard [18] applied three methods for modeling pressure and flow in carotid bifurcation. They investigate the model parameters such as flow resistance, diameter, and length of the vessel.

Klooster et. al. [19] developed a method to register MR images to allow the classification of the vessel walls to investigate the plaque components.

Using computational fluid dynamics (CFD) with single-layer and multilayer models, Lawrence-Brown et. al. [20] explore the biomechanical stress and strain behavior within the wall of the artery and its impact on plaque formation and rupture. They ran a CFD analysis to display the wall shear pressure and stress.

Cross sectional CT imaging is used by McNamara et. al. [21] to identify patients with a high carotid bifurcation who may be more likely to experience surgical problems. Since their methodology relies on hand measurements, the outcomes could vary depending on the measurements used.

The methods mentioned above are highly depending on the calculation of position e.g., volume and blood flow estimation in the carotid bifurcation. On the other hand, our research focuses the measurement of the narrowness with calculation of the angle automatically.
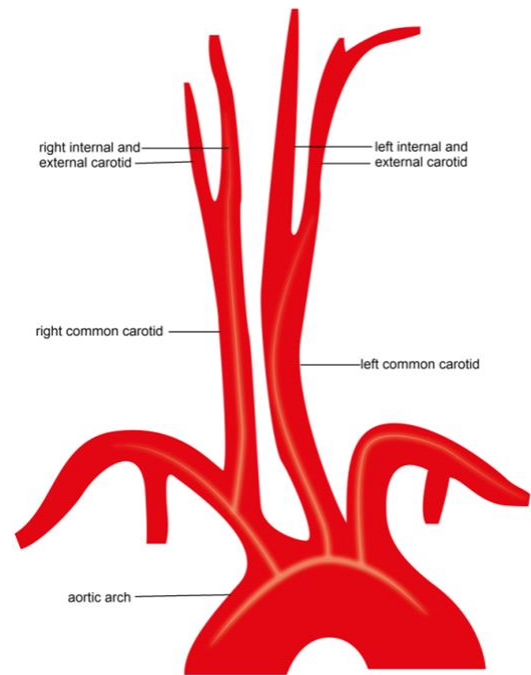
Figure 1. Carotid artery

2. Method

Cross-sectional CT imagery is used for this work. A random number of image samples is provided for each patient. The images are acquired as a cross-section in every 0.5 mm. CT images are gray-scale, and carotid vessels are visually separable from the image background, which allows running the traditional image classification methods such as ISODATA [22].

The processing chain starts with image classification. The classification approach segments the image into different categories which include the carotid vein clusters. Then, the process is followed by morphological erosion to overcome the connectivity problem of the separated veins in the images although they are separate in reality. Then, the distances between the center and the created points along the cluster boundaries are calculated to determine the circularity of the cluster.

Three parameters are used to determine the cluster if it belongs to the carotid vein class; the standard deviation of the distance values between the center and boundary points; the minimum and maximum vein section size; the maximum distance between the center points which come from the images. If three criteria meet the defined thresholds, then the corresponding cluster is selected as a carotid vein.

The areas are compared between the clusters from the successive images. The cluster which shows the maximum area difference among all the pairs is selected as the bifurcation part of the carotid. The angle is calculated between the selected vein center point and the center points from one image before and after. The processing schema can be found in Figure 2.
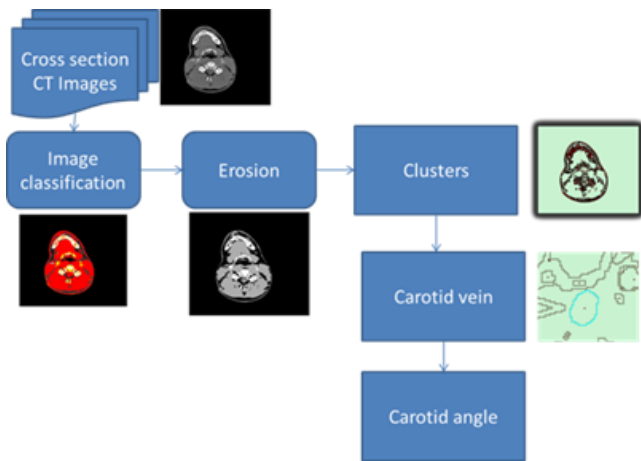
Figure 2. Processing workflow

2.1. CT Image classification

Image classification methods are widely used in urban planning, mapping applications, extraterrestrial research, forensic applications, medical image analysis, and many other topics which use imagery information. It is a technique that classifies image pixels into different categories. In medical image analysis, these categories can be listed as vessels, the brain, and other parts of the imaged part of the body.

The first step of image classification is the identification of the feature parameters with spectral characteristics. Then, feature space is divided into subspaces which do not overlap between each other. The classification is finalized with the calculation of the distance between image pixels and each subspace.

There are two types of image classification, one is unsupervised and the other is supervised image classification. In supervised classification, prior knowledge is used to determine the membership of pixels to the corresponding classes. The user selects the pixels with his own knowledge, and the algorithm estimates the parameters with this prior knowledge. There are several algorithms that are used for supervised classification. One uses a minimum distance to assign the pixel to the corresponding class. In this algorithm, the minimum distance is computed between the center of the class and the pixel value. The center of the class is calculated using the training pixel samples.

Another algorithm is maximum likelihood classification which calculates the likelihood of each pixel point by point and assigns the pixel to the corresponding class with the maximum likelihood. Maximum likelihood classification (MLC) is one of the most widely used techniques in supervised classification. Other supervised classification methods are Parallelepiped classification and Decision tree classification. Parallelepiped classification is based on a single rule while the decision tree considers different characteristics of the objects.

The unsupervised classification does not use any of the existing prior knowledge and creates clusters from the image according to its spectral characteristics. There are two kinds of unsupervised classification which are mostly used in many image processing applications which are K-means and ISODATA classification.

Both have two different aspects. K-means adjust a class each time, and each class's average value is

recalculated. ISODATA recalculates the class averages after adjusting all samples. Both are standard classification methods in any remote sensing software package.

The classical ISODATA classification algorithm has the following steps; first, the average gray value of the whole image is calculated. Secondly, the image is classified using the calculated average as the threshold value. Then, the average values are calculated for the created classes, and these values are used as new thresholds. This is repeated unless the threshold values are not changed anymore.

CT images are in gray scale, and the carotid vessels might be imaged from different directions. On the other hand, carotid vessels are separable from another background in the images also visually (Figure 3).

Figure 3. Original CT image of the bifurcation position

Finding the different vessel classes on the images is the first challenge. In its most basic form, CT imagery is grayscale. In comparison to other areas of the photos, the vessels are noticeably brighter. Using image classification methods like the ISODATA algorithm, this information is adequate to identify carotid vessels.

A collection of samples are grouped using the clustering algorithm used by ISODATA, and each sample is represented as a vector, such as $X=[x^1,...,x_N]^T$. The cluster is automatically updated after each iteration to combine comparable segments and to break segments with high standard deviations. The following equation is used to determine the sum of squared distances between each pixel and its associated cluster center:

$$\text{SSdistances} = \sum (X - C(x))^2 \qquad (1)$$

where $C(x)$ is the cluster mean for the pixel x. The Mean Squared Error (MSE), which is calculated as follows, is used to identify cluster variability.

$$\text{MSE} = \text{SS\_distances}/(N-c) \text{ b} \qquad (2)$$

where N is the number of pixels, c indicates the number of clusters, and b is the number of spectral bands, for CT images it is 1 [1,22].
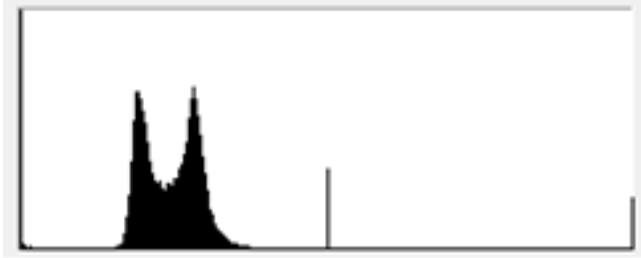

Figure 4. Histogram of CT image

As shown in Figure 4, five classes are defined with analysis of the number of peak points over the histogram. Figure 5 shows the classification result.
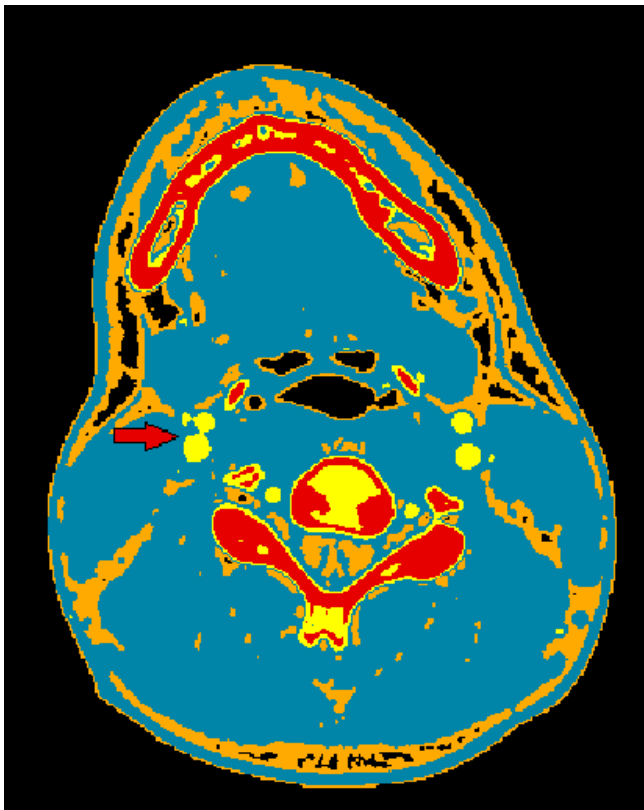

Figure 5. Classified CT image, the colors represent different clusters

2.2. Morphological operation

After clustering each section image, morphology operator erosion has been applied to the classification result to identify the vessels which are separated in reality but look connected to the images.

Morphological operations are one of the basic processes in image processing, and they apply a structuring element over the input image and create an output image. The pixel values of the input image are compared with the neighbors; the size and shape of the neighbors directly affect the result of the operations. Since the centers are the point of interest, not the boundaries, erosion is only the used approach. Erosion removes the pixels on the object boundaries by removing a number of pixels from the objects in the input image.

As seen in Figure 6, the carotid vessels are separated using erosion since the connectivity of the veins is caused by image artifacts.
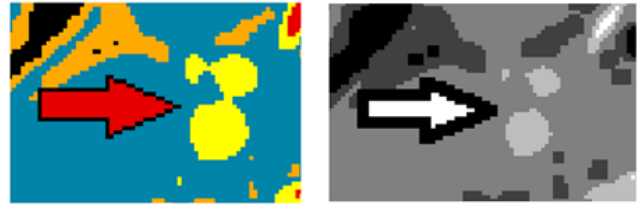

Figure 6. Before (left) and after(right) morphological operation

2.3. Identification of the carotid veins

The main idea to identify the vein clusters is using the standard deviation of the distance series between the cluster center and the vein boundary. Secondly, the veins have a certain size compared to the other clusters.

The vessels that part of the carotid artery have a circular form. The circularity can be determined with statistical analysis by calculating the standard deviation of the distance between the center and the border of the vessels. To do this, the centers of vessel clusters have been extracted, and then a series of vessel border points is generated. The distance is calculated between each border point and the center point. The center and boundary points are created using the ArcGIS software package (Figure 7). It simply extracts the centroid of the clusters and creates the points along the cluster boundaries. The gap between the points is set as a ground sample distance value.
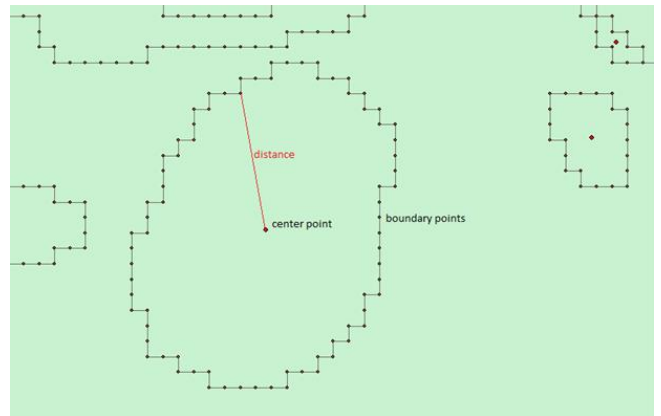

Figure 7. The center and boundary points of the extracted classes

The distance between the cluster and the boundary point is calculated as follows;

$$Di = \sqrt{(Xc - Xib)^2 + (Yc - Yib)^2} \qquad (3)$$

$$s^2 = \frac{1}{n-1} \sum_{i=1}^{n} (Di - \overline{D}) \qquad (4)$$

Xc, Yc values are coordinates of the center point, Xb and Yb values are the coordinates of the boundary point i, Di is the calculated distance with ith boundary point, s2 is variance, D is the mean value of all distances, n number of calculated distance value.

Another criterion is the area of the clusters. The maximum and minimum area thresholds are set by consideration of vein geometry.

The center points of the clusters which meet certain criteria (circularity and area) are overlaid and the distances of the center points are calculated between each other. The carotid center points always remain and they should be in a certain distance between each other after overlaying altogether on the same plane. The number of center points which are close each other is same as the number of the used image.
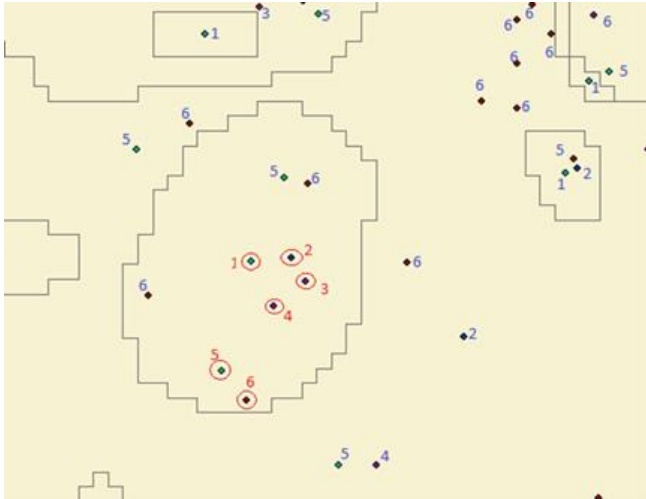
Figure 8. The image numbers of the overlaid center points

As shown in Figure 8, the center points of clusters are overlaid on the clusters image from image 1. Each point has the number of its image label.

The process starts with the first image,
- Takes the center points,
- Then check if there is any center point in its neighborhood from the next image, here image 2.
- If any point is found, then the next center point from the next image is searched in the neighborhood of the center point from the successive images.
- This process is continued until the last image.

In the Figure 8, each cluster centers are numbered with their image numbers. The number of neighbor points is same as the number of used images. This case is valid only for the carotid veins (red points in Figure 8).

2.4. Calculation of the angle

Three center points are used to calculate the carotid angle, one center point in the middle and the other two center points from the images before and after. The center point which is in the middle is selected based on the area difference between clusters. The vein cluster which has the biggest area difference between the clusters from the image after is selected as the middle, and its center point is the used center point for the angle calculation.

Let PC [1…n] center points from the same cluster from successive images. PCi is the cluster in the middle, which is the bifurcation area of the vein. Ci-1 and Ci+1 successive point those used in the angle calculation.

PCi, PCi-1, and PCi+1 are the center points from the selected clusters for calculating the angle as shown in Figure 9.
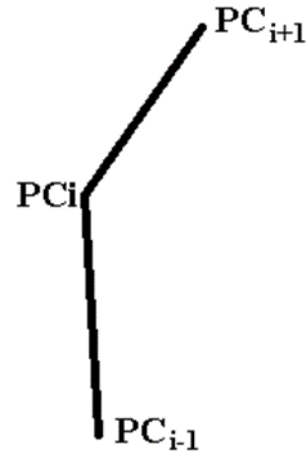
Figure 9. Illustration of carotid vein center points

The angle Ɵ is calculated using following formulas;

$$\overrightarrow{PC_{i+1}PC_i}=PC_{i+1}-PC_i \quad (5)$$

$$\overrightarrow{PC_iPC_{i-1}}=PC_i-PC_{i-1} \quad (6)$$

$$\overrightarrow{PC_{i+1}PC_i}.\overrightarrow{PC_iPC_{i-1}} = \left\|\overrightarrow{PC_{i+1}PC_i}\right\|.\left\|\overrightarrow{PC_iPC_{i-1}}\right\|.\cos\theta \quad (7)$$

$$\theta = \arccos\left(\frac{\overrightarrow{PC_{i+1}PC_i}.\overrightarrow{PC_iPC_{i-1}}}{\left\|\overrightarrow{PC_{i+1}PC_i}\right\|.\left\|\overrightarrow{PC_iPC_{i-1}}\right\|}\right) \quad (8)$$

From the image acquisition, the Z difference between each image is 0.5 mm. Z coordinate is set as 0 for the center points at the image in the bottom, other center points from the successive images have Z coordinate according to image position in the acquisition (e.g., Z coordinate for the 4the image would be 0.05 x 4= 0.2 mm).
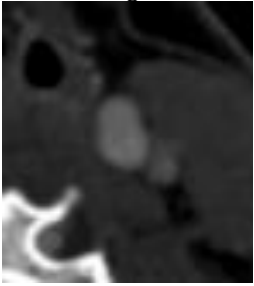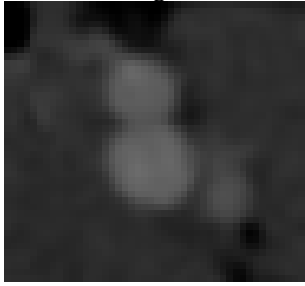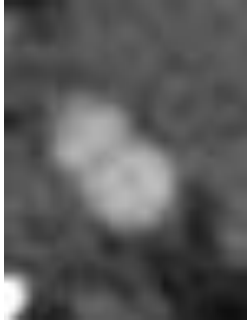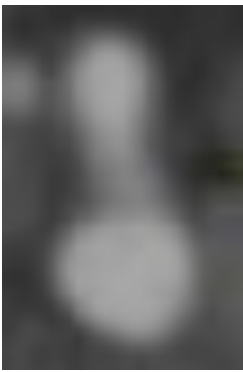
3. Results

For testing the method, 15 crosses sectional CT images from 5 different patients are used. After image classification, erosion is applied on the extracted clusters for each cross-sectional CT image.

The center and boundary points are extracted to analyze the carotid vein clusters.

Table 1 shows the three images which have been used in the angle calculation from the output of the method and the calculated a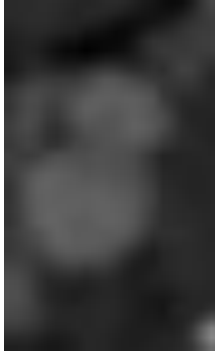ngles. On the other hand, the information regarding the position of the carotid is also achieved depending on the coordinates of the angle with respect to the image center.

Table 1. Quality evaluation of the results, only three clipped images which shows the case of bifurcation

Image 1	Image 2	Image 3	Angle (Degrees)	Position
			38.6823	Right
			43.5219	Right
			30.2174	Right
			12.1425	Left
			54.1151	Right

The results are evaluated with a visual interpretation of three image outputs from the tests. In case three images are the ones that have a bifurcation in the middle, then the result from the method has been confirmed. According to the performance evaluation, for all the tested image samples, the developed method gave the correct three images, including the bifurcation point in the middle, including giving information about the side of the carotid angle.

4. Discussion

The measurement of a carotid angle is often performed with manual measurements on the CT images by medical doctors. Even one-pixel movement during the measurement, may shift the value of the angle, therefore some methods have to be developed accordingly to allow precise measurement.

Cross-sectional CT images are used in previous studies [21]. McNamara et.al [21] used an external software to measure the carotid artery and straight-line distance to identify the high carotid bifurcation. Their measurement is performed with use of the base of skull. On the other hand, there are studies which are based on simulating blood flow in the veins [21]. Lawrence-Brown analyzes stress in carotid artery [20]. Our method uses cross sections of carotid artery which makes it different than the other methods since they derive the angle values with manual measurements on the acquired images. The evaluation is difficult since it is only possible with manual measurements, but it will be meaningless in case the calculated angles would be compared with the ones which derived on the images manually. Therefore, the only evaluation could be done with checking their position right or left. If the image coordinates of the carotid stay on the left of the image center, then the carotid was classified as left, else right.

5. Conclusion

The narrowness of carotid angle is an important factor for the human health. In general, the carotid angle is calculated with manual measurements by the medical doctors. In this study, a new method is developed to calculate the carotid angle using cross sectional CT images.

Out method automatically select the image where the bifurcation occurs, and then calculates the angle between three images, the image with a bifurcation in the middle, and one image after and other before the bifurcation.

The evaluation shows that the selected images are all correct for the calculation of the carotid angle. This allows medical doctors to select the image which has bifurcation without any mistake, and to have the carotid angle without performing any manual measurement with better accuracy.

Future work may include the reconstruction of the carotid vein to allow analyzing the blood flow in the carotid veins in 3D, the analyzing of the role of the carotid communis on the patients with stenosis.

Author contributions

Nusret Demir: Conceptualization, Methodology, Data curation, Writing-Original draft preparation, Software, Validation. **Serkan Demir:** Visualization, Investigation, Writing-Reviewing and Editing.

Conflicts of interest

The authors declare no conflicts of interest.

References

1. Demir, N., & Demir, S. (2015, May). Automated calculation of bifurcation carotid angle for analyzing the risk of carotis plaques by using carotid CT angiographic images. In *Smart Biomedical and Physiological Sensor Technology XII* (Vol. 9487, pp. 91-99). SPIE.
2. Midi, İ., & Afşar, N. (2010). İnme risk faktörleri. *Klinik gelişim*, *10*(1), 1-14.
3. Bouthillier, A., Van Loveren, H. R., & Keller, J. T. (1996). Segments of the internal carotid artery: a new classification. *Neurosurgery*, *38*(3), 425-433.
4. Adams, R. D., Victor, M., Ropper, A. H., & Daroff, R. B. (1997, July). Principles of neurology. Neuropsychiatry, Neuropsychology & Behavioral Neurology, 10(3), 220
5. Autret, A., Saudeau, D., Bertrand, P. H., Pourcelot, L., Marchal, C., & De Boisvilliers, S. (1987). Stroke risk in patients with carotid stenosis. *The Lancet*, *329*(8538), 888-890.
6. Inzitari, D., Eliasziw, M., Gates, P., Sharpe, B. L., Chan, R. K., Meldrum, H. E., & Barnett, H. J. (2000). The causes and risk of stroke in patients with asymptomatic internal-carotid-artery stenosis. *New England Journal of Medicine*, *342*(23), 1693-1701.
7. Ringelstein, E. B., Koschorke, S., Holling, A., Thron, A., Lambertz, H., & Minale, C. (1989). Computed tomographic patterns of proven embolic brain infarctions. *Annals of Neurology: Official Journal of the American Neurological Association and the Child Neurology Society*, *26*(6), 759-765.
8. European Carotid Surgery Trialists Collaborative Group. (1991). MRC European Carotid Surgery Trial: interim results for symptomatic patients with severe (70-99%) or mild (0-29%) carotid stenosis. *Lancet*, *337*, 1235-1243.
9. Mayberg, M. R., & Winn, H. R. (1995). Endarterectomy for asymptomatic carotid artery stenosis: resolving the controversy. *JAMA*, *273*(18), 1459-1461.
10. Dix, J. E., Evans, A. J., Kallmes, D. F., Sobel, A. H., & Phillips, C. D. (1997). Accuracy and precision of CT angiography in a model of carotid artery bifurcation stenosis. *American journal of neuroradiology*, *18*(3), 409-415.

11. Suinesiaputra, A., de Koning, P. J., Zudilova-Seinstra, E., Reiber, J. H., & van der Geest, R. J. (2012). Automated quantification of carotid artery stenosis on contrast-enhanced MRA data using a deformable vascular tube model. *The International Journal of Cardiovascular Imaging*, *28*(6), 1513-1524.

12. Kefayati, S., & Poepping, T. L. (2010, January). 3-D flow characterization and shear stress in a stenosed carotid artery bifurcation model using stereoscopic PIV technique. In *2010 Annual International Conference of the IEEE Engineering in Medicine and Biology* (pp. 3386-3389). IEEE.

13. Fisher, M. (2012). Geometry is destiny for carotid atherosclerotic plaques. *Nature Reviews Neurology*, *8*(3), 127-129.

14. Stroud, J. S., Berger, S. A., & Saloner, D. (2002). Numerical analysis of flow through a severely stenotic carotid artery bifurcation. *Journal of Biomechanical Engineering, 124*(1), 9-20.

15. Cebral, J. R., Yim, P. J., Löhner, R., Soto, O., & Choyke, P. L. (2002). Blood flow modeling in carotid arteries with computational fluid dynamics and MR imaging. *Academic radiology*, *9*(11), 1286-1299.

16. Tan, F. P. P., Soloperto, G., Bashford, S., Wood, N. B., Thom, S., Hughes, A., & Xu, X. Y. (2008). Analysis of flow disturbance in a stenosed carotid artery bifurcation using two-equation transitional and turbulence models. *Journal of biomechanical engineering*, *130*(6), 061008

17. Wong, K. K., Thavornpattanapong, P., Cheung, S. C., Sun, Z., & Tu, J. (2012). Effect of calcification on the mechanical stability of plaque based on a three-dimensional carotid bifurcation model. *BMC cardiovascular disorders*, *12*(1), 1-18.

18. Gul, R., & Bernhard, S. (2015). Parametric uncertainty and global sensitivity analysis in a model of the carotid bifurcation: Identification and ranking of most sensitive model parameters. *Mathematical biosciences*, *269*, 104-116.

19. van 't Klooster, R., Staring, M., Klein, S., Kwee, R. M., Kooi, M. E., Reiber, J. H., ... & van der Geest, R. J. (2013). Automated registration of multispectral MR vessel wall images of the carotid artery. *Medical physics*, *40*(12), 121904.

20. Lawrence-Brown, M., Stanley, B. M., Sun, Z., Semmens, J. B., & Liffman, K. (2011). Stress and strain behaviour modelling of the carotid bifurcation. *ANZ Journal of Surgery*, *81*(11), 810-816.

21. McNamara, J. R., Fulton, G. J., & Manning, B. J. (2015). Three-dimensional computed tomographic reconstruction of the carotid artery: identifying high bifurcation. *European Journal of Vascular and Endovascular Surgery*, *49*(2), 147-153.

22. Ridler, T. W., & Calvard, S. (1978). Picture thresholding using an iterative selection method. *IEEE trans syst Man Cybern*, *8*(8), 630-632.